Density of interface states, electron traps, and hole traps as a function of the nitrogen density in SiO_2 on SiC

John Rozen,[1,a)] Sarit Dhar,[1,b)] M. E. Zvanut,[2] J. R. Williams,[3] and L. C. Feldman[1,4]
[1]*Department of Physics and Astronomy, and Institute of Nanoscale Science and Engineering, Vanderbilt University, Nashville, Tennessee 37235, USA*
[2]*Department of Physics, University of Alabama at Birmingham, Birmingham, Alabama 35294, USA*
[3]*Department of Physics, Auburn University, Auburn, Alabama 36849, USA*
[4]*Institute of Advanced Materials, Devices and Nanotechnology, Rutgers University, Piscataway, New Jersey 08854, USA*

(Received 19 February 2009; accepted 14 April 2009; published online 22 June 2009)

Nitridation of the SiO_2/SiC interface yields a reduction in interface state density, immunity to electron injection, as well as increased hole trapping. It is shown that the accumulation of nitrogen at the oxide/semiconductor interface is solely responsible for these three effects. The evolution of the density of interface states, electron traps, and hole traps is measured in metal-oxide-semiconductor capacitors as a function of the nitrogen content which is varied by adjusting the gate oxide NO annealing time. A rate equation is derived to model the change in the interface state density, observed at various energy levels, in terms of nitrogen binding cross-sections. While the generation of acceptor interface states upon electron injection is suppressed after minimum N incorporation, the density of oxide hole traps appears to scale linearly with the amount of nitrogen. The origin and the properties of the N-induced hole traps resembles those of the defects responsible for enhanced negative bias temperature instability observed in nitrided silicon devices. It is proposed that the binding of nitrogen is not exclusively driven by the passivation of defects at the semiconductor surface but also results in the formation of a silicon oxynitride layer redefining the interface. © *2009 American Institute of Physics*. [DOI: 10.1063/1.3131845]

I. INTRODUCTION

Silicon carbide oxide-based devices have the potential to surpass silicon technology in high-power, high-frequency, and high-temperature applications.[1,2] The larger carrier saturation velocity and thermal conductivity of SiC indeed allow for better energy efficiency under such operating conditions. Many efforts have been dedicated to the improvement of the interface between SiC and its thermal gate oxide, SiO_2, mainly in order to reduce the series resistance in the ON state of metal-oxide-semiconductor field-effect transistors (MOSFETs) by increasing the channel mobility. The most common technique used to improved the inversion mobility is the introduction of nitrogen at the interface via post-oxidation anneal (POA) in nitric (NO) or nitrous oxide (N_2O).[3,4] Even though there is still substantial room for improvement, such POAs have become standard and scrutiny now turns toward the impact of nitridation on the long-term reliability of devices.

The reliability of SiC semiconductor devices may be characterized in a variety of ways. Among them, time-dependent dielectric breakdown (TDDB) measurements which yield the mean time to failure (MTTF) of the devices is most common. After nitridation of the SiO_2/SiC interface, the MTTF of oxides subject to electron injection increases, and is higher than the MTTF resulting from hole leakage.[5,6] Unfortunately, TDDB is set to probe catastrophic dielectric failure and does not quantify the voltage instabilities induced by the progressive carrier trapping which ultimately lead to oxide breakdown. To better understand the physical mechanisms inducing the degradation of the gate dielectric in SiC devices, we have used other accelerated techniques such as internal photoemission (IPE), Fowler–Nordheim (FN) tunneling, and x-ray irradiation, in parallel with capacitance-voltage (*CV*) measurements to monitor the trapped charge as a function of the injected charge in the oxide. We recently reported that, although high-temperature NO annealing improves the quality of the SiO_2/4H-SiC interface by reducing the interface state density (D_{it}) and by suppressing electron-induced interface state generation,[7] the incorporation of nitrogen in the dielectric also yields a large density of hole traps.[8,9] While these results can explain the TDDB findings, they highlight an important shortcoming of the standard NO process.

While the buildup of positive charge is an obvious concern in *p*-channel SiC devices in the ON state, it can also occur in the preferred *n*-channel MOSFETs. In the latter case, the holes originate from the accumulation layer in the OFF state. Even at zero bias they can access traps several Ångstroms within the oxide via quantum tunneling. This phenomenon will be amplified if a negative gate bias is applied to ensure minimal drain current. Moreover, the use of SiC devices at high temperature (e.g., 150 °C) promotes carrier injection via both tunneling and emission.[10,11] It should therefore be obvious that the impact of nitrogen on the hole

[a)]Also at the Central Research Institute of Electric Power Industry, Yokosuka-shi, Kanagawa 240-0196, JP. Author to whom correspondence should be addressed. Electronic mail: john.rozen@vanderbilt.edu.
[b)]Present address: Cree Inc., Research Triangle Park, North Carolina 27709, USA.

 © 2009 American Institute of Physics

Author complimentary copy. Redistribution subject to AIP license or copyright, see http://jap.aip.org/jap/copyright.jsp

TABLE I. Successive fabrication steps used for each of the samples.

Samples	O_2 @ 1150 °C	Ar @ 1150 °C	Ar @ 1175 °C	NO @ 1175 °C	$N_2:O_2$ @ 1175 °C
Ar_30	7 h	30 min	⋯	⋯	⋯
N2:O2_120	7 h	30 min	⋯	⋯	120 min
NO_0	7 h	30 min	120 min	⋯	⋯
NO_7.5	7 h	30 min	112.5 min	7.5 min	⋯
NO_15	7 h	30 min	105 min	15 min	⋯
NO_30	7 h	30 min	90 min	30 min	⋯
NO_60	7 h	30 min	60 min	60 min	⋯
NO_120	7 h	30 min	⋯	120 min	⋯

trapping is a major concern as it can lead to accelerated degradation of all SiC oxide-based devices under certain operating conditions.

Positive charge buildup in the dielectric due to negative gate bias and temperature has been widely studied in silicon *p*MOSFETs and is referred to as negative bias temperature instability (NBTI).[12] In Si devices, nitrogen may be incorporated in the oxide as well, not to reduce the interface state density (which is achieved by hydrogen passivation), but to limit dopant diffusion and reduce gate leakage.[13,14] However, as in SiC devices, nitridation can lead to electron immunity and increased hole trapping.[15–19] The latter is commonly observed during NBTI measurements. It is therefore useful to see if the properties of nitrided oxides on either SiC or Si can be interpreted within the same framework.

The nature of the electron and hole traps in SiO_2 on SiC is the subject of this manuscript. Trap densities in the gate dielectric of 4H-SiC metal-oxide-semiconductor (MOS) capacitors are characterized as a function of the amount of nitrogen incorporated in SiO_2. The nitrogen content is controlled by the duration of the NO anneal that follows the thermal growth of the gate oxide. The resulting nitrogen concentrations at the interface are measured by secondary ion mass spectroscopy (SIMS). Charge injection of electrons and holes is performed using photoemission, FN tunneling, and x-ray irradiation. To complement this study, electron spin resonance (ESR) measurements were performed in order to trace the atomic configuration of the charged defects. Correlations are made between the reduction in D_{it}, the generated interface states, and the trapped hole densities, quantities measured by the *CV* technique. An analytical expression is derived to model the evolution of the D_{it} at various energy levels. On one hand, it is found that the amount of interface states generated during electron injection is very sensitive to NO exposure as they vanish after the shortest anneals. On the other hand, the density of positive charge trapped during hole injection and x-ray irradiation (under positive gate bias) increases linearly with the amount of nitrogen. These observations indicate that electron immunity is related to the passivation of particular precursor interface defects that are preferred N binding sites, while the NO-induced hole trap density is a property of the nitrogen binding configurations in the oxide, implying that each nitrogen atom could act as a hole trap and that their presence in the near-interface region is probably undesirable. Control samples show that neither the higher temperature used for nitridation nor the slow reoxidation taking place during the NO anneal can explain the observed behaviors, confirming that the nitrogen incorporated at the SiO_2/SiC interface is solely responsible. The chemistry of N is discussed and it is proposed that nitridation does more than passivate defects as it could redefine the interface region altogether by forming an oxynitride.

II. EXPERIMENTS

A. Sample preparation

The substrates used in the experiments are *n*-type 4H-SiC with a deposited epitaxial layer ($N \simeq 5 \times 10^{15}$ cm^3) purchased from Cree Inc. They were dipped in TCE, acetone, methanol, and BOE (buffered HF), prior to performing the standard RCA cleaning steps. Oxidation was achieved in flowing O_2 at 1150 °C for 7 h and followed by an Ar anneal at the same temperature for 30 min, yielding an oxide thickness of the order of 50 nm on the polished (0001) Si-face, as determined by *CV* and ellipsometry. The quartz tube furnace was then cooled down in Ar to allow for the distinct processing of each sample. Nitridation was subsequently performed via NO annealing at 1175 °C. In order to incorporate varying amounts of nitrogen, the NO exposure was adjusted between 0 and 120 min. The thermal budget was maintained constant for all nitrided samples by using Ar prior to the introduction of NO, so that they all spent a total time of 2 h at temperature. These samples are labeled NO_*x* (where *x* is the NO exposure time in min). In addition, two control samples were fabricated. To test the impact of the higher temperature, they were removed after the 1150 °C Ar anneal (never exposed to 1175 °C, nor nitric oxide). One of them was then further oxidized at 1175 °C in a flowing $N_2:O_2$ (9:1) mixture to characterize the impact of the slow reoxidation taking place during NO anneals ($\simeq$1 nm SiO_2 grown per hour), without incorporating nitrogen. These two samples are labeled Ar_30 and N2:O2_120, respectively. The successive thermal processing steps are summarized for all samples in Table I. Semitransparent Al gate contacts ($\leq$30 nm thick and 500 μm diameter) were evaporated to form MOS capacitors on the (0001) Si-face. Finally, a drop-etch using BOE was performed to remove the oxide grown on the back side and sputtered Au, or colloidal Ag paste, was used to ensure good Ohmic contact to the substrate.

Author complimentary copy. Redistribution subject to AIP license or copyright, see http://jap.aip.org/jap/copyright.jsp

B. Nitrogen profiling

The profile and the density of incorporated nitrogen in NO-annealed samples were determined at EAG laboratories (Hightstown, NJ 08520, USA) using SIMS. The nitrogen concentrations are calibrated against a thermal silicon dioxide standard that has been ion-implanted with nitrogen. The depth scale has been calibrated against a crater measurement on the same standard sample.

Because the ionization yield of emerging atoms differs from the bulk standard at the studied oxide/silicon carbide interface, a cross-calibration with other methods was needed to estimate the error on the integrated N count. Most importantly, it should be noted that the relative concentrations of incorporated nitrogen extracted from the various samples, yielding the presented analysis, are very accurate. The depth resolution and the precision of the SIMS technique are discussed more thoroughly in Sec. III A.

C. Carrier injection

Charge injection into the gate oxide was achieved at room temperature by three different techniques. (i) Electron injection by IPE was performed at low fields using the focused radiation of a 100 W mercury lamp to emit free carriers from the negatively biased metal gate ($V_g = -10$ V, leading to an electric field in the dielectric $|E_{ox}| < 2$ MV/cm).[7] (ii) Holes were injected via FN tunneling from the semiconductor kept in inversion by a negative gate bias and a low intensity UV light ($E_{ox} \simeq -6$ MV/cm).[8] (iii) Electron-hole pairs were generated by a 10 keV x-ray source, while a positive bias was maintained on the gate to attract the electrons and push the holes to the SiO_2/SiC interface ($V_g = 7.5$ V and $E_{ox} \simeq 1.5$ MV/cm).[8,9]

CV measurements were performed at room temperature to monitor the D_{it} and the flatband voltage V_{fb} during charge injection. The D_{it}, between 0.2 and 0.6 eV from the SiC conduction band edge, was extracted from quasistatic (0.5 V/s) and high-frequency (100 kHz) *CV* curves taken simultaneously from accumulation to depletion using a Keithley model 82 setup.[20] The change in flatband voltage upon injection ΔV_{fb} was monitored by the shift in the high-frequency *CV* curve, measured at flatband capacitance, and was renormalized to the shift a 50 nm oxide would yield, so that all samples can be directly compared. The effective density of trapped charge is calculated as $C_{ox}\Delta V_{fb}/q$ where C_{ox} is the oxide capacitance and q is the elementary charge. This results in a negative value for positive trapped charge and in a positive value for negative trapped charge.

In order to optimize the measurements, electron injection via photoemission, hole injection via FN tunneling and intermediary *CV* characterization were automated and performed on up to three devices simultaneously. The setup designed for these experiments is illustrated in Fig. 1. High-frequency switch cards (Keithley 7062) are used together with a controller (Keithley 705) to alternate *CV* measurements and charge injection. The high-frequency *CV* sweeps (Keithley 590) are performed on each device sequentially from accumulation to depletion. During the injection steps, the required bias (Keithley 236) is applied to the devices, which

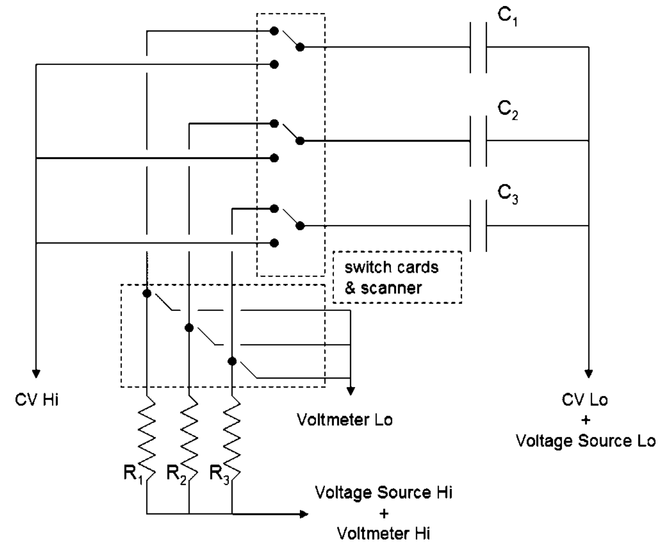

FIG. 1. Schematic of the electrical connections of the designed automated injection setup. Capacitance-voltage measurements and monitored charge injection can be performed in sequence. Up to three devices are tested simultaneously. A custom LABVIEW program controls the units and processes the data.

are connected in parallel. The total injected charge for each device is obtained by integrating the current calculated from the potential differences measured sequentially by a digital multimeter (Keithley 706) across resistors (100 MΩ) connected in series. The value of the resistors was chosen to provide the required accuracy for currents of the order of nanoampere
($\simeq 500$ nA/cm^2), while maximizing the fraction of voltage dropped across tested devices (>90%). During *CV* measurements, the low intensity UV lamp was kept on when performing FN hole injection experiments, but the high intensity UV beam was blocked by a shutter when performing photoemission of electrons. A custom LABVIEW program was implemented to control the units and process the data.

D. Electron spin resonance

For ESR measurements, oxides on the (000–1) C-face of semi-insulating 6H-SiC and the (001) face of Si were grown in the conditions described above. Some of them were then annealed for 2 h in NO at 1175 °C, yielding an SiO_2 thickness of about 275 and 425 nm on SiC and Si, respectively. *X*-band ESR measurements were made at 30 K. The *g*-value, characteristic of the ESR signal, was calculated from the applied field at resonance, and the relative number of centers was determined by the comparison of the peak-to-peak amplitude of the ESR signal.[21]

ESR was used primarily to monitor the number of positively charged oxygen vacancies (E' centers).[22,23] Since oxygen vacancies are typically neutral and undetectable by ESR is as-grown films, the defects were charged by irradiation at room temperature to 5 or 10 Mrad (SiO_2) using the 10 keV x-ray source.

Note that for ESR measurements, the thicker C-face SiC oxides were irradiated so that the signal from centers charged after irradiation could be maximized. Although one has to keep in mind that the devices were fabricated on the Si-face

Author complimentary copy. Redistribution subject to AIP license or copyright, see http://jap.aip.org/jap/copyright.jsp

of 4H-SiC, we expect the ESR results to be relevant because we are interested in comparing the properties of the oxide bulk and of the near interface with and without nitridation. Indeed, while one might expect the SiC faces and polytypes to produce a quantitative difference in the results, the qualitative comparison used here between irradiated ESR samples and electrically injected devices should be valid.[24]

III. RESULTS AND DISCUSSION

A. Kinetics of the nitrogen uptake

The evolution of the nitrogen profile and concentration in the samples exposed to NO at high temperature were monitored as a function of annealing time. The SIMS data for samples NO_7.5, NO_30, and NO_120 is shown in Fig. 2. The peaks correspond to the nitrogen profiles, N concentrations, are labeled on the left axis. The carbon (C) and oxygen (O) concentrations are plotted in arbitrary units (right axis). In order to have the three nitrogen profiles on the same graph, their respective C and O signal were aligned so that the position of the peaks can be studied relative to the SiO_2/SiC interface.

In all cases, the nitrogen is located at the interface, as previously reported.[25–28] Furthermore, it can be seen that the relative position of the peaks remains constant. This indicates that, during the slow reoxidation associated with the NO annealing (see details below), the nitrogen peak moves with the interface toward the semiconductor as more Si and C atoms are consumed by the formation of SiO_2 ($\simeq 1$ nm/h). Oxides annealed using N_2O lead to the same observation.[25,29] Other techniques such as NH_3 annealing and plasma nitridation incorporate nitrogen throughout the SiO_2, which reveals that the kinetics of NO and N_2O anneals are unique.[30–32] In addition, for NO and N_2O, the incorporation rates scale with the oxidation rates when comparing nitrogen uptake on the Si-face, *a*-face, C-face of SiC, and on silicon.[28] All this suggests that the nitrogen uptake results from the dissociation of NO at the oxide/semiconductor interface during NO and N_2O anneals.

The full width at half maximum (FWHM) of the SIMS nitrogen peaks is constant for all measured annealing times. It implies that the extent of the region in which nitrogen is incorporated remains the same. Note that the extracted width

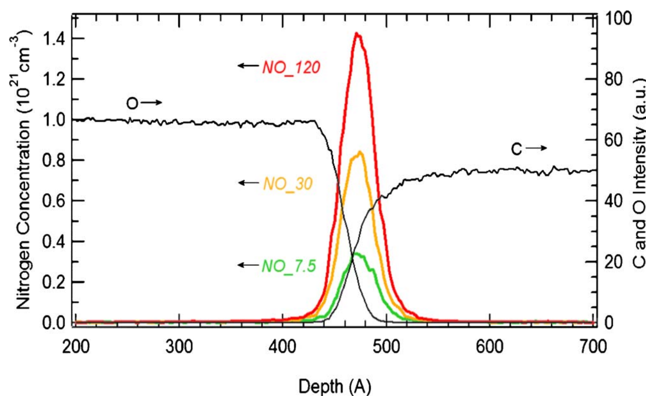

FIG. 2. (Color online) SIMS profiles for the samples annealed in NO for 7.5, 30, and 120 min.

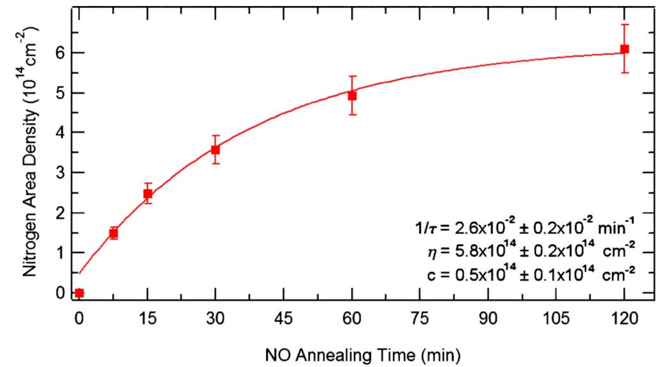

FIG. 3. (Color online) N area density as a function of NO annealing time calculated by integrating the SIMS N signal. The curve is the fit by Eq. (1), the resulting values of the parameters are listed.

of $\simeq 3$ nm is limited by the SIMS technique as there are several processes impacting its depth resolution: collision cascades cause intermixing of the ions at the interface and artificial profile broadening, the stress and chemical nature of the interface can affect the sputtering rate of the primary beam, and the ionization yield of atoms emerging from that region can change. In fact, it has been shown from electron energy-loss spectroscopy (EELS) that the nitrogen is confined to within at most 1.2 nm of the SiO_2/SiC interface, the resolution limit of the EELS technique.[27,28] The localized dissociation of NO, the passivation of defects, and/or the release of interfacial stress could explain the accumulation of nitrogen in that region only.

In order to study the evolution of the nitrogen incorporation rate, the N area density η (in atoms/cm^2) was extracted as a function of the NO annealing time t (in minutes) from the SIMS data (Fig. 3). The values were obtained by subtracting the background noise at detection limit ($\simeq 10^{18}$ cm^{-3} seen in the sample NO_0) prior to integrating the N signal. In previous experiments, the absolute values of the area density deduced from SIMS were estimated to be accurate within a factor of two by a cross-calibration with nuclear reaction analysis (NRA) and medium energy ion scattering (MEIS).[33,34] This may be due to peculiar particle-solid interactions at the oxide/semiconductor interface as mentioned above. Note that this absolute concentration uncertainty affects neither the analysis nor the resulting conclusions made in this manuscript; the relative error for each point, i.e., the reproducibility, being within 5%.

The data can be modeled by a first-order rate equation of the form

$$\eta[t] = \eta^*(1 - e^{-t/\tau}) + c, \quad (1)$$

where η^* is the nitrogen area density at saturation, $1/\tau$ is an effective binding rate (in min^{-1}), and c is an offset constant. The equilibrium density of N at the interface comes in part from a balance between incorporation and removal. Indeed, it has been demonstrated that the nitrogen introduced at the SiO_2/SiC interface via NO and N_2O anneals is not stable against reoxidation,[29] i.e., it is removed in the presence of oxygen. This affects the kinetics of the nitrogen uptake because there is always a source of oxygen during NO and N_2O exposure at high temperature.[33] Therefore, the parameters η^*

Author complimentary copy. Redistribution subject to AIP license or copyright, see http://jap.aip.org/jap/copyright.jsp

and τ depend explicitly on the gaseous concentration of both NO and oxygen at the interface, as well as on the binding and removal rates of nitrogen.[11,28]

The fit of the data by Eq. (1) for $t>0$, shown in Fig. 3, yields values for the effective binding rate and c that are about 2.6×10^{-2} min^{-1} and 0.5×10^{14} cm^{-2}, respectively. The nitrogen saturation density is estimated at approximately 5.8×10^{14} cm^{-2}, in fair agreement with the previously published values which were obtained by a variety of techniques,[25,26,33,34] including MEIS which yields $1.1\pm0.6\times10^{15}$ cm^{-2}. Note that the maximum amount of nitrogen that can be incorporated at the SiO_2/SiC interface using N_2O in similar conditions is about an order of magnitude less.[25] This correlates nicely with the ratio of O_2 to NO at 1175 °C which is estimated to be 0.5 and 3 during NO and N_2O annealing, respectively, implying a faster reoxidation in the latter case.

B. Impact of temperature and slow reoxidation

In this section, the effects of the higher temperature used during NO exposure and of the slow reoxidation that occurs in parallel are studied in an attempt to isolate the role of the nitrogen on the electrical properties of the oxide and of the interface. In order to do so, the D_{it}, as well as the hole and electron trapping behaviors, are monitored in four different samples: sample Ar_30 (processed at 1150 °C, never exposed to NO), sample N2:O2_120 (POA at 1175 °C in N_2:O_2 mixture, 9:1, for 2 h), sample NO_0 (POA at 1175 °C in Ar for 2 h), and sample NO_120 (POA at 1175 °C in NO for 2 h).

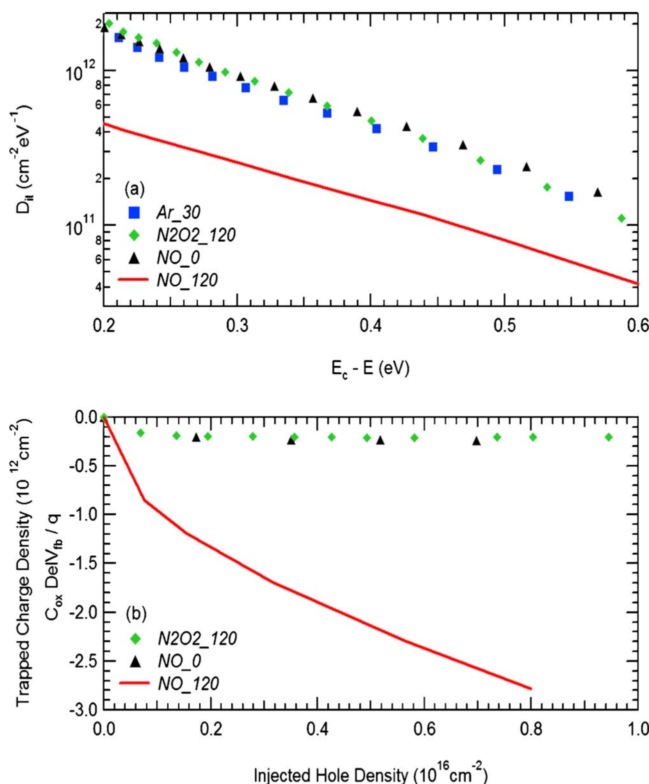

FIG. 4. (Color online) Density of interface states (a) and of trapped positive charge (b) in the control samples and in the one annealed in NO for 2 h. The temperature and the slow reoxidation have no significant effect on either properties, only the nitrogen incorporated during the NO anneal does.

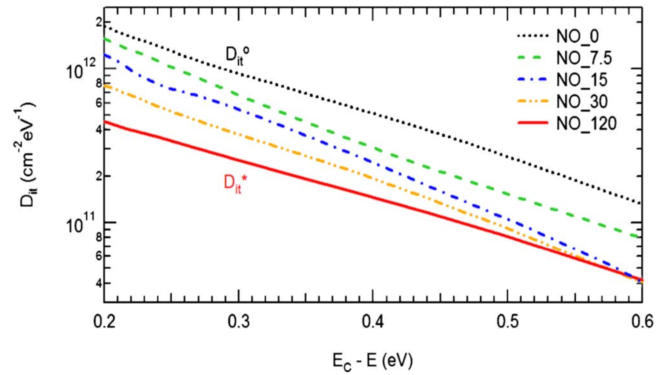

FIG. 5. (Color online) Density of interface states of the control sample (2 h Ar at 1175 °C) and of the ones annealed for 7.5, 15, 30, and 120 min in NO. D^0_{it} and D^*_{it} refer to the D_{it} prior to NO annealing and at N saturation, respectively.

The interface state densities of these samples are plotted in Fig. 4(a). It can be seen that neither the temperature nor the reoxidation impacts the D_{it} as much as the NO anneal. This is in agreement with plasma nitridation experiments from which the nitrogen alone is shown to achieve NO-like D_{it}.[30] In Fig. 4(b), the effective trapped charge ($C_{ox}\Delta V_{fb}/q$) is shown as a function of the injected hole density. The NO-annealed oxides are found to possess a hole trap density much larger than the one of any other oxide. Finally, the generation of interface states observed upon electron injection, and the associated negative charge trapping, is suppressed only after NO exposure (not shown).

It is therefore concluded that the incorporation of nitrogen at the SiO_2/SiC interface is solely responsible for the reduction in D_{it}, for the electron immunity, and for the increased hole trap density. The data presented in the following sections are interpreted in these terms.

C. Progressive reduction in interface state density

The interface state density between 0.2 and 0.6 eV from the SiC conduction band edge is plotted in Fig. 5 for different NO annealing times. The upper curve corresponds to the base D_{it} obtained from sample NO_0 annealed in Ar at 1175 °C for 2 h (D^0_{it}). It can be seen that the high-temperature NO treatment is efficient at progressively reducing the amount of electrically active levels throughout the monitored energy window.

Because the impact on the D_{it} of the temperature and of the slow reoxidation have been shown to be negligible compared to the observed impact of NO anneals, this reduction is attributed to the passivation, the alteration, and/or the removal of defects by nitrogen binding at the oxide/semiconductor interface. Theory suggests that nitrogen can indeed substitute for threefold coordinated atoms or bind at defect sites, which reduces the D_{it} in the upper part of the 4H-SiC band gap.[35] These defects could be of various nature and therefore have different energy levels, explaining the efficiency of nitrogen over a wide energy range. For example, single carbon interstitials at the interface, or silicon suboxide bonds in the oxide (of various lengths) are expected to have levels close to the conduction band edge. Also, carbon "clusters" at the interface, e.g., a six-atom aggregate resulting

Author complimentary copy. Redistribution subject to AIP license or copyright, see http://jap.aip.org/jap/copyright.jsp

from a split C interstitial at a Si site in SiC, are expected to have levels located deeper in the gap. All these defects are theoretically sensitive to nitrogen. Nevertheless, we note that the N effect may not be only atomic in nature, but also associated with the formation of a new dielectric in the immediate vicinity of the interface.

The difference between D_{it}^0 and the D_{it} at N saturation (D_{it}^*) is shown in Fig. 6(a). It reveals that N removes more levels toward the conduction band edge. This is mostly because their density is higher prior to NO annealing. Indeed, the reduction in the D_{it} normalized by D_{it}^0, Fig. 6(b), indicates that the efficiency of nitrogen is comparable throughout the monitored energy window, as it removes about 70% of all levels. This suggests that the corresponding defects are of similar nature or at least that they are affected the same way by N incorporation. However, the shape of the curve indicates that levels within 0.3 eV of the conduction band could be associated to a distinct category of atomic configurations. Actually, it has been observed that the D_{it} of unpassivated samples rises very sharply in that region[36] and reaches a value of several times of $10^{13}\ \text{cm}^{-2}\,\text{eV}^{-1}$. These shallow states are thought to originate mostly from Si–Si suboxide bonds and to be very sensitive to nitrogen incorporation.[37] Another important parameter to extract is the total density of levels removed after NO annealing between 0.2 and 0.6 eV. This is done by integrating the curve in Fig. 6(a). It yields a value of approximately $7.6\times10^{11}\ \text{cm}^{-2}$ which is only about 0.1% of the N area density at saturation. Even when considering the shallow states and the levels in the rest of the band gap, it appears that there are two orders of magnitude more nitrogen incorporated than there are electrically active defects to passivate. This surprisingly large number will be discussed below.

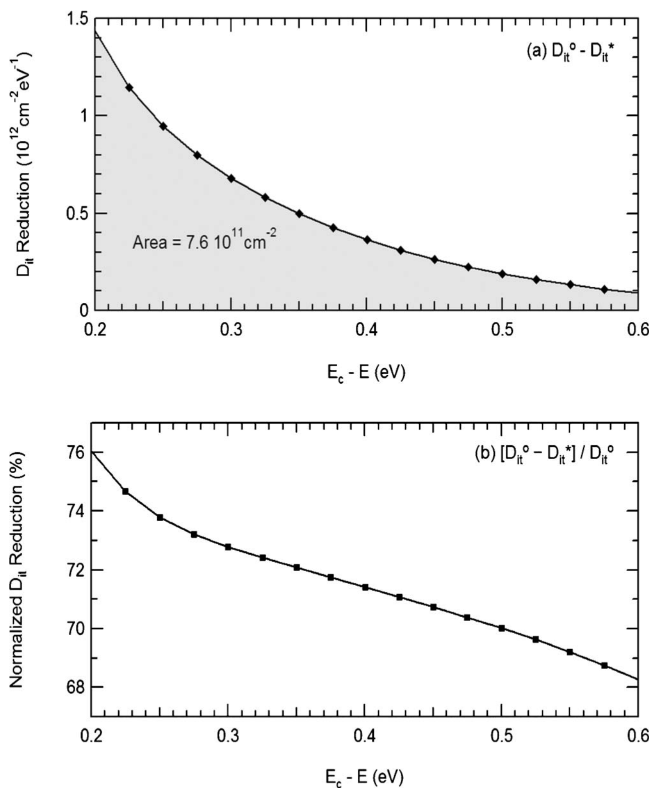

FIG. 6. D_{it} reduction (a) and normalized D_{it} reduction (b) after nitrogen saturation at the SiO_2/SiC interface.

The evolution of the D_{it} at specific levels is shown as a function of the nitrogen area density in Figs. 7(a)–7(e). This allows a determination of the impact of N incorporation at different energies. A passivation model was previously derived by McDonald *et al.*[26] It assumed the reduction in size of carbon clusters which progressively moved the defect levels deeper in the band gap. This does not seem to apply to the data reported here as there is no evidence of a step formation in D_{it} versus η (the nitrogen area density) for deeper levels, which motivated the model. On the contrary, the present results show that the density of deeper levels saturate faster than shallow states upon N incorporation. It should be noted that the processing of the samples was different in the two experiments. McDonald *et al.*[26] used a wet oxidation to grow the oxides, as well as a reoxidation process; they report a higher D_{it}^0 and D_{it}^* which is likely related to the presence of other dominant defects.

Before attempting to relate the amount of nitrogen to the evolution of the D_{it} observed here, it should be recognized that distinct atomic configurations lead to distinct energy levels. Accordingly, a model that determines where the incorporated nitrogen is most likely to bind is derived. For each type of binding site, the binding rate is expected to be proportional to a cross-section s_j (in cm^2) and to the density of available such sites D_j (in cm^{-2}). It should also be inversely proportional to the sum $\sum_i s_i D_i$ over all competing locations, i.e., over the binding sites of different nature. This leads to the differential equation

$$\frac{dD_j[\eta]}{d\eta} = -\frac{s_j\{D_j[\eta]-D_j^*\}}{\sum_i s_i\{D_i[\eta]-D_i^*\}}, \tag{2}$$

where D_j^* is the remaining density of available sites when η reaches η^*, the N area density at saturation. It can be solved for all sites by defining an average cross-section

$$s_{\text{av}} = \frac{\sum_i s_i(D_i - D_i^*)}{\sum_i (D_i - D_i^*)}, \tag{3}$$

noting that

$$\sum_i (D_i - D_i^*) = \eta^* - \eta. \tag{4}$$

Using Eqs. (3) and (4), Eq. (2) becomes

$$\frac{dD_j}{d\eta} = -\frac{s_j(D_j - D_j^*)}{s_{\text{av}}(\eta^* - \eta)}, \tag{5}$$

which can be solved exactly with the boundary condition $D_j[0]=D_j^0$;

$$D_j[\eta] = (D_j^0 - D_j^*)\left(\frac{\eta^* - \eta}{\eta^*}\right)^{s_j/s_{\text{av}}} + D_j^*. \tag{6}$$

When D_j corresponds to an atomic configuration that is electrically active, it can be interpreted as the density of levels at a given energy E_j, s_j becoming a passivation cross-

Author complimentary copy. Redistribution subject to AIP license or copyright, see http://jap.aip.org/jap/copyright.jsp

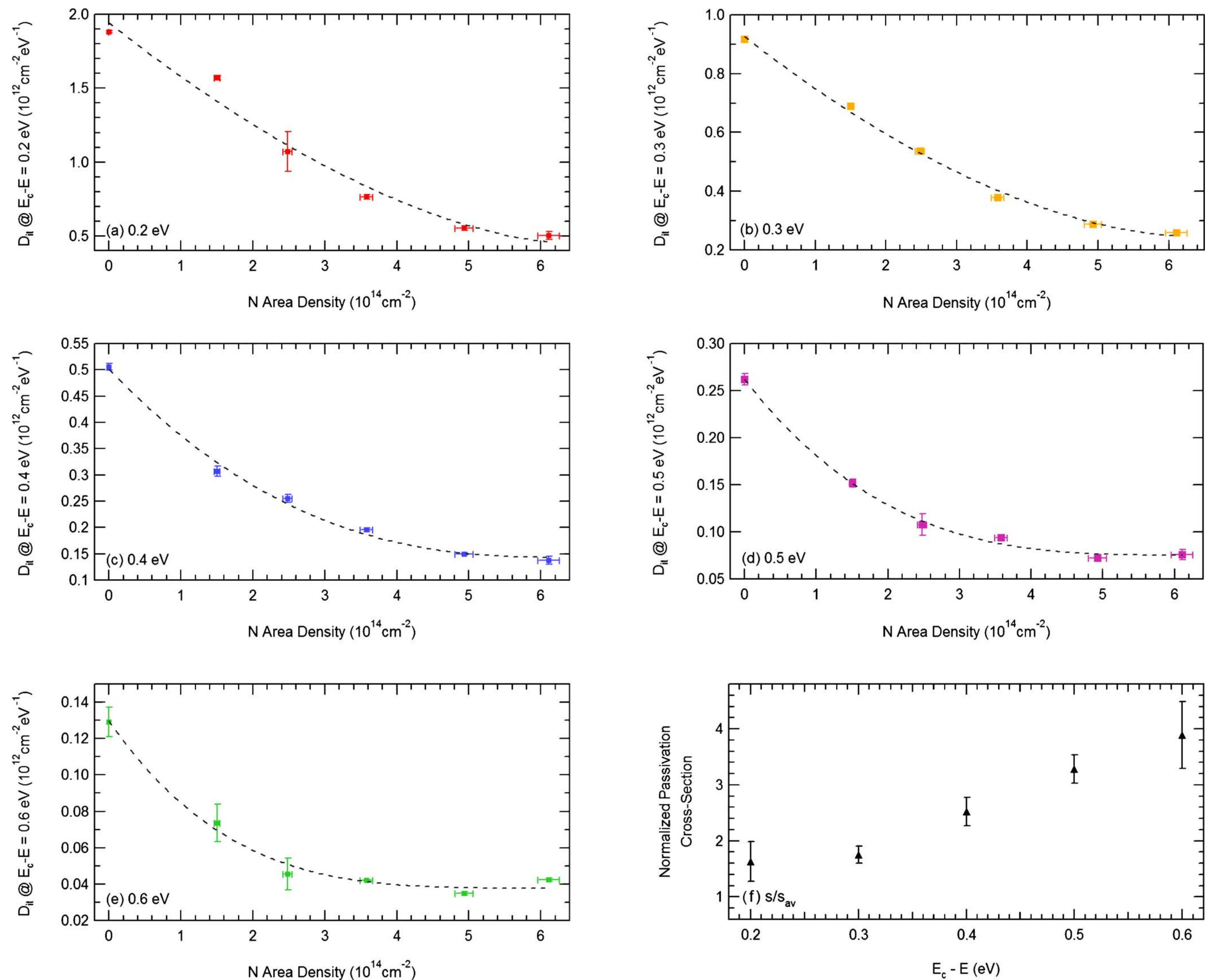

FIG. 7. (Color online) [(a)–(e)] Evolution of the D_{it} at different energy levels as a function of the area density of nitrogen incorporated by NO annealing. The amount of nitrogen required to achieve saturation seems to be less for levels deeper in the gap, it varies from $\simeq 5\times 10^{14}$ cm^2 at $E_c-E=0.2$ eV to $\simeq 3\times 10^{14}$ cm^2 at $E_c-E=0.6$ eV. The dashed lines are fits by Eq. (6). (f) Normalized passivation cross-sections extracted form the fits.

section. The derived model can then be used to study the observed impact of nitrogen on the density of interface states, with the hypothesis that N atoms remove levels within the studied energy window without introducing any. Indeed, Eq. (6) is found to successfully model the evolution of the D_{it} at each energy level considered in Figs. 7(a)–7(e). The obtained normalized cross-sections (s_j/s_{av}) are shown in Fig. 7(f). Their increasing values for levels deeper in the band gap correspond to the earlier saturation of the D_{it} at these energies. It indicates that, although the density of corresponding defects is small prior to nitridation when compared to the rest of the band gap, they could be binding sites favored by N. Once again, a distinction can be made between the levels within 0.3 eV of the conduction band edge and the ones deeper in the band gap. Indeed, ones between 0.2 and 0.3 eV have similar passivation cross-sections, further indicating that they relate to a separate category of defects.

Note that if more than one incorporated nitrogen atom is required to remove an electrically active interface level, say αN, the ultimate D_{it} reduction at E_j would correspond to $(D_j^0-D_j^*)/\alpha$. Could this explain why there are two orders of magnitude more N incorporated than there are interface states removed from the gap? It is hard to conceive, because it would not only imply that there is a progressive redistribution of the energy levels, which is not observed here between 0.2 and 0.6 eV, but also that apparently up to 100 N atoms would be needed to remove a single defect level, assuming N targets only defects inducing D_{it}.

Instead, it is proposed that the binding of nitrogen is not exclusively driven by the passivation of defects at the semiconductor interface but also results in the formation of a silicon oxynitride layer ($\eta^*\simeq 1/2$ monolayer of Si_3N_4) extending into the oxide. Nitrogen can indeed be incorporated in SiO_2, regardless of the interface state density, as evidenced by the similar characteristics of the nitrogen uptake in SiO_2 on Si and on SiC.[25] Moreover, it can bind in the bulk of the oxide following plasma or NH_3 nitridation, regardless of the substrate.[30–32] This correlates with our theoretical calculations predicting that N can disturb a perfect oxide by inserting within a Si–O–Si bridge.[8] In any case, this large amount

Author complimentary copy. Redistribution subject to AIP license or copyright, see http://jap.aip.org/jap/copyright.jsp

of nitrogen not associated with defect passivation is expected to be detrimental to the SiO_2/SiC interface like it is to the SiO_2/Si interface. Indeed, it enhances hole trapping in both cases, as discussed in a following section.

D. Suppression of electron-induced interface state generation

In this section and the next, the effective trapped charge density N_{eff} (in cm^{-2}) is calculated from the flatband voltage shifts $(C_{ox}\Delta V_{fb}/q)$ upon injection in several capacitors. In order to perform an average for each nitrogen content, the following analytical expression is used to fit the data from individual devices:

$$N_{eff}[\rho] = N_1(1 - e^{-\sigma_1\rho}) + N_2(1 - e^{-\sigma_2\rho}), \tag{7}$$

where ρ is the injected charge density (in cm^{-2}). This equation, which assumes that there are two kinds of trapping events occurring in parallel, is found to accurately describe the experimental curves. The two trap area densities are N_1 and N_2, they have a capture cross-section equal to σ_1 and σ_2, respectively (in cm^2).

The effective charge densities trapped upon electron injection are plotted in Fig. 8 for devices having three different nitrogen contents $(0,\ 2.5\times10^{14}$, and $5\times10^{14}\ cm^{-2})$ corresponding to various NO exposure times (0, 15, and 60 min). It can be seen that in the unpassivated sample (NO_0) the trapped charge shows no sign of saturation within the monitored window. This has been associated with electron-induced generation of acceptor states at the SiO_2/SiC interface.[7,38] This phenomenon is immediately suppressed, even for the shortest NO annealing times, as the curves extracted from samples NO_15 and NO_60 are identical within statistical errors. In these samples, only background electron trapping, i.e., from the oxide bulk, is thought to remain. From Eq. (7), the density of bulk traps is estimated to be around $1.2\times10^{11}\ cm^{-2}$ and to have a trapping cross-section of about $3.9\times10^{-16}\ cm^2$, in good agreement with the previous measurements. The cross-section associated with interface state generation is found to be about $2\times10^{-17}\ cm^2$.

Because nitridation leads to the suppression of interface state generation, we have proposed that the nitrogen affects precursor defects susceptible to electron trapping. Potential atomic configurations that could explain such behavior were listed in Ref. 7. We now observe that the suppression of interface state generation is achieved for $\eta \ll \eta^*$, indicating that such precursor defects would be preferred nitrogen binding sites. Note that this is also the case for atomic configurations inducing deep interface states, as indicated by their larger passivation cross-sections extracted in the previous section. Accordingly, such defects could also be related to interface state generation upon electron injection in unpassivated oxides.

E. Increase in oxide hole trap density

The effective charge density trapped upon FN hole injection is plotted in Fig. 9 for various nitrogen contents. The background trapping observed in the unpassivated sample (NO_0) is found from Eq. (7) to correspond to a trap density of around $2.3\times10^{11}\ cm^{-2}$ which has a hole capture cross-section of about $1.2\times10^{-15}\ cm^2$. As previously established,[8,9] it can clearly be seen that the introduction of nitrogen at the interface leads to additional hole traps. The corresponding capture cross-section is estimated between 10^{-17} and $10^{-16}\ cm^2$. The large density of hole traps resulting from the standard (2 h) NO process can lead to a flatband voltage shift of more than −7 V in a 50 nm oxide, noting that no saturation of the positive trapped charge can be observed. This is a concern for the reliability of both *n*-channel and *p*-channel SiC MOSFETs as mentioned earlier, prompting us to further characterize the NO-related trap.

Note that the amount of N-induced hole traps scales with the NO annealing time. This is emphasized in Fig. 10 where the effective density of charge trapped after injecting 10^{16} holes/cm^2 is plotted as a function of the N area density η (filled symbols). The trapping resulting from 5 Mrad (SiO_2) under positive gate bias is shown as well (empty symbols). Both curves reveal a linear dependence of the hole trap density on η up to N saturation in the oxide. It is important to realize that this linear scaling refers to the nitrogen content and not to the NO annealing time. This is another indication that hole trapping is induced by the binding of nitrogen in the interfacial region and not by a secondary process, as established in Sec. III B.

The absolute hole trap density at η^* is difficult to estimate because positive charge saturation is not observed and because of possible field-induced detrapping. However, a lower value can be set at $3\times10^{12}\ cm^{-2}$. This, and the linear

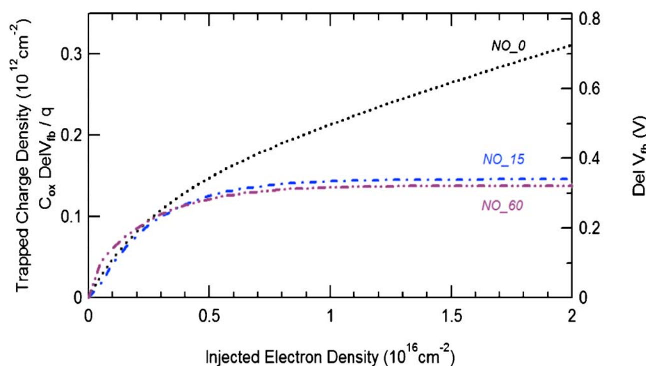

FIG. 8. (Color online) Effective charge trapped upon electron injection in an unpassivated oxide (NO_0) and in oxides annealed for 15 and 60 min in NO.

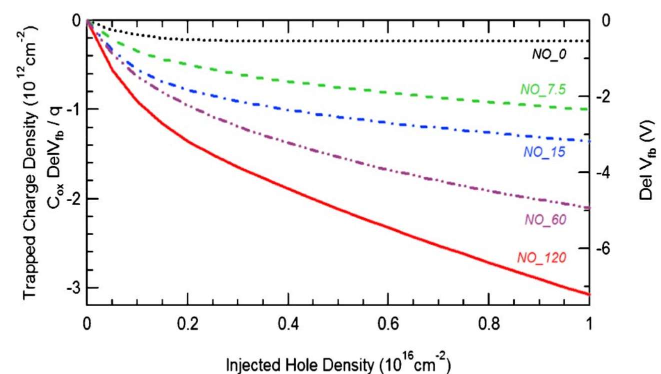

FIG. 9. (Color online) Effective trapped charge upon hole injection in oxides annealed for various times in NO.

Author complimentary copy. Redistribution subject to AIP license or copyright, see http://jap.aip.org/jap/copyright.jsp

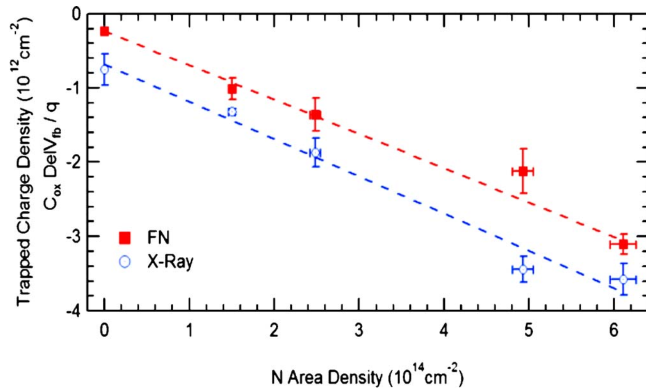

FIG. 10. (Color online) Effective trapped charge after the injection of 10^{16} holes/cm^2 by Fowler-Nordham tunneling (FN) tunneling and after 5 Mrad (SiO_2) exposure under positive bias (x-ray), as a function of the N area density.

relationship of the trap density with η, suggests that the hole traps induced by nitrogen do not correspond to the passivation of any single level within 0.2–0.6 eV from the 4H-SiC conduction band edge studied in Sec. III C. This should not come as a surprise since the positive trapped charge is stable against the formation of an electron accumulation layer in *n*-type SiC substrates, suggesting that the atomic configurations inducing trapping exist more than a few Ångstroms away from the semiconductor (tunneling distance) and extend into the oxide. Since we know that nitrogen must be involved in hole trapping, we speculate that these traps extend up to about 1.2 nm into the oxide, as it corresponds to a maximum width of the oxynitride transition layer set by EELS.[27,28]

So far, two observations made during these experiments have suggested that nitrogen binding is not uniquely driven by true interface defect passivation: (i) the nitrogen density is two orders of magnitude larger than the integrated D_{it} reduction over the band gap and (ii) the N-related hole traps extend away from the interface. But the most powerful argument indicating that nitrogen binding is related to the SiO_2 more than to the semiconductor maybe comes from the observations made on silicon oxide-based devices. Not only is there formation of an oxynitride in both cases, but it is well known in Si technology that nitrogen increases the oxide hole trap density, as evidenced by NBTI measurements.[16–19] In fact, those densities are found to be linearly proportional as well.[16] Therefore, some aspects of the oxide near-interfaces on both semiconductors after, and possibly before, nitridation appear to be similar. Accordingly, it is likely that the N-related hole traps originate from the same atomic configurations in oxides grown on Si and SiC. Thus, we can attempt to join the partial understandings of both systems toward a better characterization of common near-interface defects.

In this instance, the two tools we can use to identify the N-induced defects are ESR spectroscopy and first-principle calculations. Suboxide Si–Si bonds (oxygen vacancies) are defects known to extend within the oxide and to behave as hole traps. Indeed, they have been deemed partially responsible for NBTI at the SiO_2/Si interface.[23] As they are E' center precursors, their density can be monitored by ESR measurements. Even though these atomic configurations do not involve nitrogen, it has to be established whether or not the enhanced hole trapping after nitridation of the oxide, observed on both Si and SiC, can be explained by a simultaneous increase in E' precursors. From the ESR spectra taken on irradiated oxides on Si [Fig. 11(a)] and SiC [Fig. 11(b)], we find that the E' signal intensity (magnified in the insets) decreases between the as-oxidized and NO-annealed samples. Note that the measured ESR signals correspond to the derivative of absorption peaks, so that the decrease in E' centers is revealed by the damped variation around resonance ($\simeq$3361 G). This demonstrates that NO annealing actually reduces the number of E' centers in oxides grown on both semiconductors. Furthermore, ESR scans taken over a larger magnetic field range reveal none of the other charged oxygen vacancy centers attributed to SiO_2.[39,40] Consequently, the ESR analysis suggests that after nitridation, Si–Si suboxide bonds are not the dominant hole trap. According to the conclusions made above, we should instead be looking for an atomic configuration containing nitrogen. In fact, using ESR, Campbell *et al.*[41,42] have recently shown that the majority of

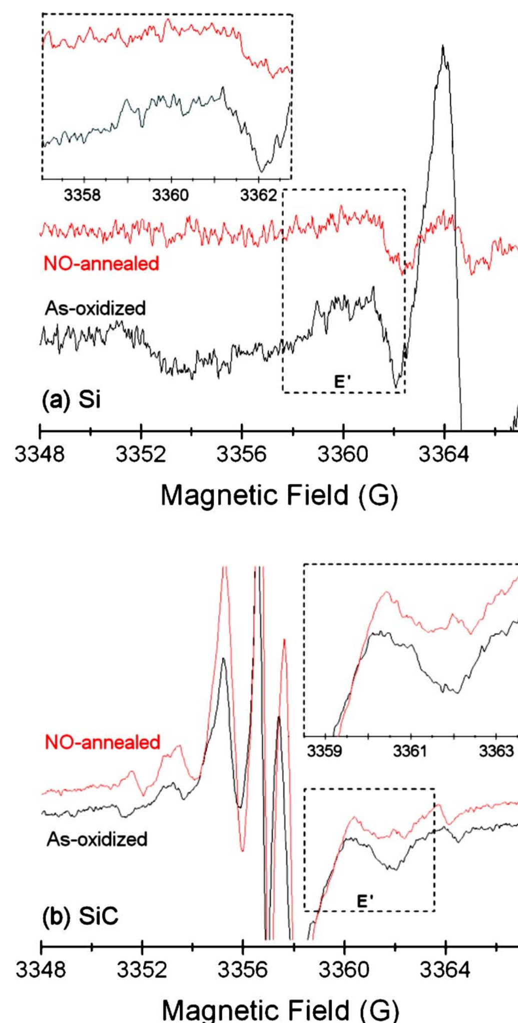

FIG. 11. (Color online) ESR spectra of irradiated oxides on Si (a) and SiC (b), where the lower (black) spectrum and the upper (red) spectrum were measured, respectively before and after NO POA. The dashed boxes enclose the E' signal (centered at $\simeq$3361 G), which is magnified in the insets. The remaining features in the spectra originate from the substrates.

Author complimentary copy. Redistribution subject to AIP license or copyright, see http://jap.aip.org/jap/copyright.jsp

the positive trapped charge in SiO_2 on Si after nitridation resides in K_N centers; Si atoms back-bonded to some N atoms in the near- interface SiO_xN_y transition region. Because the near-interface on SiC is proposed to be similar, it is reasonable to assume that the same N-induced configurations are also responsible for enhanced hole trapping in NO-annealed oxides on SiC.

Since the band gap of pure silicon nitride is entirely contained within the one of silicon dioxide, it should be expected that any intermediate stoichiometry between SiO_2 and Si_3N_4, hence SiO_xN_y, will induce energy levels accessible to excess carriers in the dielectric. This hand waving argument is indeed confirmed by theoretical simulation results published recently.[8] Because the first-principle calculations were performed in supercells representing amorphous SiO_2, those results are expected to remain valid regardless of the substrate. It was concluded that N atoms and NO molecules could insert in Si–Si suboxide bonds and Si–O–Si bridges leading to an oxygen protrusion. In the latter case, it would correspond to nitrogen converting a perfect oxide into an oxynitride. The binding of nitrogen in SiO_2 is expected to induce a lone-pair state close to the valence band edge of 4H-SiC (within the valence band of Si). This level is predicted to act as a hole trap, which could be the origin of the enhanced hole trapping after nitridation.

If the Si–NO–O–Si and Si–NO–Si bridges, resulting from nitridation of SiO_2, are precursor defects leading to the ESR signal observed by Campbell *et al.*[41,42] after hole capture, one can imagine a trapping mechanism such as

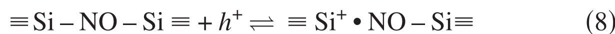

$$\equiv \mathrm{Si} - \mathrm{NO} - \mathrm{Si} \equiv + h^{+} \rightleftharpoons \equiv \mathrm{Si}^{+} \bullet \mathrm{NO} - \mathrm{Si} \equiv \qquad (8)$$

with the charged silicon bonded to some other nitrogen atoms in the SiO_xN_y transition layer. It is indeed possible that after the hole is captured by the lone-pair state of the nitrogen, the positive charge becomes localized on a Si atom, weakening the corresponding Si–N bond. Because the number of K_N centers is expected to be lower than our present detection limit, more extensive ESR studies need to be pursued to determine if such configurations indeed exist in NO-annealed oxides on either Si or SiC.

IV. CONCLUSIONS

It has been shown that following high-temperature NO anneals of SiO_2 on SiC, the incorporated nitrogen is detected exclusively at the oxide/semiconductor interface. The N area density saturates around 6×10^{14} cm^{-2}, a value thought to originate from the competition between N binding at host sites and N removal during the slow reoxidation occurring in parallel. The kinetics have been modeled by a first-order rate equation.

The higher temperature of the NO process and the resulting slow reoxidation have been shown to have little impact on the properties of the oxide and of the interface. It is therefore concluded that the binding of nitrogen at the interface is solely responsible for the decrease in D_{it}, for the electron immunity, and for the increase in hole trap density.

Although it is not clear whether nitrogen truly passivates defects or modifies the structure of the interface altogether, the evolution of the density of interface states at a given level as a function of the N area density has been shown to be well described by a derived passivation model up to the minimum D_{it}. The reduction rates are proportional to a binding cross-section and to the amount of active levels present prior to nitrogen incorporation, which ultimately leads to the removal of about 70% of the states between 0.2 and 0.6 eV from the 4H-SiC conduction band edge. The density of deeper levels seems to be minimized faster, which indicates that there is no progressive lowering of the energy of defect levels within the SiC band gap when the described processing steps are used.

On one hand, the interface state generation upon electron injection is suppressed after the smallest N area density is introduced; it suggests that it is related to the passivation, the removal, or the modification, of precursor defects at the interface. On the other hand, the incorporation of nitrogen progressively increases the hole trap density up to the largest N content achievable. The amount of hole traps and their generation rate by N shows that these traps do not originate from the removal of any active levels within the 0.2–0.6 eV window. In addition, the density of E' centers has been shown to be reduced after the NO annealing, which suggests that SiO_2 oxygen vacancies are not related to the enhanced hole trapping. Because the positive trapped charge is stable against the formation of an electron accumulation layer, it is thought that the hole traps originate from the formation of a SiO_xN_y layer extending about 1.2 nm into the oxide. It is proposed that this layer could redefine the near-interface region and also affect the D_{it}, as opposed to a simple model in which N atoms only targets certain defects for passivation.

Even though the exact nature of all the nitrogen bonding configurations following NO exposure remains to be identified, it is clear that part of them, related or not with defect passivation at the interface, play a role in the positive charge buildup in the oxide during hole injection. Accordingly, it is reasonable to assume that the same nitrogen-induced levels are responsible for enhancing the positive trapped charge observed during NBTI measurements on nitrided SiO_2 on silicon. In particular, the hole trap densities scale linearly with the N content in both systems. In the case of Si, nitrogen can be moved away from the interface by a reoxidation process to reduce NBTI without negating the N-related enhanced oxide properties. However, in the case of SiC, the presence of nitrogen at the interface is necessary to increase the channel mobility of oxide-based devices. If the inversion mobility increase follows the D_{it} reduction after NO up to N saturation, the resulting hole trapping would seem unavoidable, and the tolerance on the stability of device characteristics would have to determine the amount of nitrogen required. In order to establish this, we are in the process of studying the scaling between the inversion mobility and the nitrogen content at the interface introduced by NO.

ACKNOWLEDGMENTS

We would like to thank the following colleagues: Professor D. M. Fleetwood, Professor R. D. Schrimpf, and Dr. S. K. Dixit for their help with the implementation and interpretation of the x-ray irradiation experiments, Professor S. T.

Author complimentary copy. Redistribution subject to AIP license or copyright, see http://jap.aip.org/jap/copyright.jsp

Pantelides and Professor S. Wang for fruitful discussions with respect to theory, Professor V. V. Afanas'ev for his help with the carrier injection measurements, Professor J. A. Cooper for insights on device properties, and Dr. A. B. Hmelo for his laboratory supervision.

This work was made possible by the support and encouragements of Dr. A. J. Lelis (ARL) and Dr. T. Burke (TACOM/TARDEC), through U.S. Army Research Grant Nos. W911NF-07-2-0046 and W56HZV-06-C-0228.

[1]J. A. Cooper, Jr., M. R. Melloch, R. Singh, A. Agarwal, and J. W. Palmour, IEEE Trans. Electron Devices **49**, 658 (2002).
[2]B. J. Baliga, *Silicon Carbide Power Devices* (World Scientific, Singapore, 2006).
[3]G. Y. Chung, C. C. Tin, J. R. Williams, K. McDonald, M. D. Ventra, S. T. Pantelides, L. C. Feldman, and R. A. Weller, Appl. Phys. Lett. **76**, 1713 (2000).
[4]H. Li, S. Dimitrijev, H. B. Harrison, and D. Sweatman, Appl. Phys. Lett. **70**, 2028 (1997).
[5]S. Krishnaswami, M. K. Das, A. K. Agarwal, and J. W. Palmour, Mater. Res. Soc. Symp. Proc. **815**, J8.4 (2004).
[6]S. Krishnaswami, S.-H. Ryu, B. Heath, A. Agarwal, J. Palmour, B. Geil, A. Lelis, and C. Scozzie, Mater. Sci. Forum **527–529**, 1313 (2006).
[7]J. Rozen, S. Dhar, S. Wang, S. T. Pantelides, V. V. Afanas'ev, J. R. Williams, and L. C. Feldman, Appl. Phys. Lett. **91**, 153503 (2007).
[8]J. Rozen, S. Dhar, S. K. Dixit, F. O. Roberts, H. L. Dang, S. Wang, S. T. Pantelides, V. V. Afanas'ev, J. R. Williams, and L. C. Feldman, J. Appl. Phys. **103**, 124513 (2008).
[9]S. K. Dixit, S. Dhar, J. Rozen, S. Wang, R. D. Schrimpf, D. M. Fleetwood, S. T. Pantelides, J. R. Williams, and L. C. Feldman, IEEE Trans. Nucl. Sci. **53**, 3687 (2006).
[10]R. Singh and A. R. Hefner, Solid-State Electron. **48**, 1717 (2004).
[11]J. Rozen, Ph.D. thesis, Vanderbilt University, 2008.
[12]D. K. Schroder and J. A. Babcock, J. Appl. Phys. **94**, 1 (2003).
[13]T. Sasaki, K. Kuwazawa, K. Tanaka, J. Kato, and D.-L. Kwong, IEEE Electron Device Lett. **24**, 150 (2003).
[14]A. E. Islam, G. Gupta, S. Mahapatra, A. T. Krishnan, K. Ahmed, F. Nouri, A. Oates, and M. A. Alam, Tech. Dig. - Int. Electron Devices Meet. **2006** 1.
[15]P. T. Lai, J. P. Xu, and Y. C. Cheng, IEEE Trans. Electron Devices **46**, 2311 (1999).
[16]S. S. Tan, T. P. Chen, C. H. Ang, and L. Chan, Microelectron. Reliab. **45**, 19 (2005).
[17]D. S. Ang and S. Wang, IEEE Electron Device Lett. **27**, 914 (2006).
[18]J. B. Yang, T. P. Chen, S. S. Tan, C. M. Ng, and L. Chan, J. Electrochem. Soc. **154**, G255 (2007).
[19]A. E. Islam, H. Kufluoglu, D. Varghese, S. Mahapatra, and M. A. Alam, IEEE Trans. Electron Devices **54**, 2143 (2007).
[20]E. H. Nicollian and J. R. Brews, *Metal Oxide Semiconductor, Physics and Technology* (Wiley, New York, 1982).
[21]J. A. Weil, J. R. Bolton, and J. E. Wertz, *Electron Paramagnetic Resonance, Elementary Theory and Practical Applications* (Wiley, New York, 1994).
[22]F. J. Feigl, W. B. Fowler, and K. L. Yip, Solid State Commun. **14**, 225 (1974).
[23]P. M. Lenahan and P. V. Dressendorfer, J. Appl. Phys. **55**, 3495 (1984).
[24]V. V. Afanas'ev and A. Stesmans, Appl. Phys. Lett. **69**, 2252 (1996).
[25]K. McDonald, M. B. Huang, R. A. Weller, L. C. Feldman, J. R. Williams, F. C. Stedile, I. J. R. Baumvol, and C. Radtke, Appl. Phys. Lett. **76**, 568 (2000).
[26]K. McDonald, R. A. Weller, S. T. Pantelides, L. C. Feldman, G. Y. Chung, C. C. Tin, and J. R. Williams, J. Appl. Phys. **93**, 2719 (2003).
[27]K. C. Chang, Y. Cao, L. M. Porter, J. Bentley, S. Dhar, L. C. Feldman, and J. R. Williams, J. Appl. Phys. **97**, 104920 (2005).
[28]S. Dhar, L. C. Feldman, K. C. Chang, Y. Cao, L. M. Porter, J. Bentley, and J. R. Williams, J. Appl. Phys. **97**, 074902 (2005).
[29]K. Chatty, V. Khemka, T. P. Chow, and R. J. Gutmann, J. Electron. Mater. **28**, 161 (1999).
[30]H. Yano, Y. Furumoto, T. Niwa, T. Hatayama, Y. Uraoka, and T. Fuyuki, Mater. Sci. Forum **457-460**, 1333 (2004).
[31]A. Yankova, L. Do Thank, and P. Balk, Solid-State Electron. **30**, 939 (1987).
[32]G. J. Dunn and P. W. Wyatt, IEEE Trans. Nucl. Sci. **36**, 2161 (1989).
[33]K. McDonald, L. C. Feldman, R. A. Weller, G. Y. Chung, C. C. Tin, and J. R. Williams, J. Appl. Phys. **93**, 2257 (2003).
[34]S. Dhar, Y. W. Song, L. C. Feldman, T. Isaacs-Smith, C. C. Tin, J. R. Williams, G. Chung, T. Nishimura, D. Starodub, T. Gustafsson, and E. Garfunkel, Appl. Phys. Lett. **84**, 1498 (2004).
[35]S. Wang, S. Dhar, S.-r. Wang, A. C. Ahyi, A. Franceschetti, J. R. Williams, L. C. Feldman, and S. T. Pantelides, Phys. Rev. Lett. **98**, 026101 (2007).
[36]V. V. Afanas'ev, A. Stesmans, M. Bassler, G. Pensl, and M. J. Schulz, Appl. Phys. Lett. **76**, 336 (2000).
[37]V. V. Afanas'ev, A. Stesmans, F. Ciobanu, G. Pensl, K. Y. Cheong, and S. Dimitrijev, Appl. Phys. Lett. **82**, 568 (2003).
[38]V. V. Afanas'ev, A. Stesmans, M. Bassler, G. Pensl, M. J. Schulz, and C. I. Harris, J. Appl. Phys. **85**, 8292 (1999).
[39]A. Stesmans, F. Scheerlinck, and V. Afanas'ev, Appl. Phys. Lett. **64**, 2282 (1994).
[40]J. F. Conley, Jr., P. M. Lenahan, H. L. Evans, R. K. Lowry, and T. J. Morthorst, J. Appl. Phys. **76**, 2872 (1994).
[41]J. P. Campbell, P. M. Lenahan, C. J. Cochrane, A. T. Krishnan, and S. Krishnan, IEEE Trans. Device Mater. Reliab. **7**, 540 (2007).
[42]J. P. Campbell, P. M. Lenahan, A. T. Krishnan, and S. Krishnan, Appl. Phys. Lett. **91**, 133507 (2007).

Author complimentary copy. Redistribution subject to AIP license or copyright, see http://jap.aip.org/jap/copyright.jsp